Surface-phase superconductivity in a Mg-deficient V-doped $MgTi_2O_4$ spinel

A. Rahaman,[1,2] T. Paramanik,[1,3] B. Pal,[4,*] R. Pal,[4] P. Maji,[1] K. Bera,[5] S. Mallik,[5] D. K. Goswami,[1] A. N. Pal,[4] and D. Choudhury[1,†]

[1]*Department of Physics, Indian Institute of Technology Kharagpur, Kharagpur 721302, India*
[2]*Department of Physics, Yogoda Satsanga Palpara Mahavidyalaya, Palpara 721458, India*
[3]*Department of Physics, School of Sciences, National Institute of Technology Andhra Pradesh, Tadepalligudem 534102, India*
[4]*Department of Condensed Matter and Materials Physics, S. N. Bose National Centre for Basic Sciences, Sector III, Block JD, Salt Lake, Kolkata 700106, India*
[5]*School of Nanoscience and Technology, Indian Institute of Technology Kharagpur, Kharagpur 721302, India*

(Received 5 August 2022; revised 31 May 2023; accepted 5 June 2023; published 15 June 2023)

Around 50 years ago, $LiTi_2O_4$ was reported to be the only spinel oxide to exhibit a superconducting transition with the highest $T_c \approx 13.7$ K. Recently, $MgTi_2O_4$ has been found to be another spinel oxide to reveal a superconducting transition with $T_c \approx 3$ K, however, its superconducting state is realized only in thin film superlattices involving $SrTiO_3$. We find that a V-doped $Mg_{1-x}Ti_2O_4$ phase, which gets stabilized as a thin surface layer on top of a nearly stoichiometric and insulating V-doped $MgTi_2O_4$ bulk sample, exhibits high-temperature superconductivity with $T_c \approx 16$ K. The superconducting transition is also confirmed through a concomitant sharp diamagnetic transition immediately below T_c. The spinel phase of the superconducting surface layer is conformed through grazing-incidence x-ray diffraction and micro-Raman spectroscopy. A small shift of the sharp superconducting transition temperature (~4 K) with the application of a high magnetic field (up to 9 T) suggests a very high critical field for the system, ~25 T. Thus, V-doped $Mg_{1-x}Ti_2O_4$ exhibits the maximum T_c among spinel superconductors and also possesses a very high critical field.

DOI: 10.1103/PhysRevB.107.245124

I. INTRODUCTION

The identification of new superconducting materials is an extremely fascinating and challenging task in the field of condensed matter physics. In this regard, spinel compounds, which are well known for exhibiting a plethora of functional properties due to a strong coupling between its charge, spin, orbital, and lattice degrees of freedom, are rarely found to be superconductors. Around five decades ago (1967), some of the sulfo- and selenospinels were successfully synthesized with superconducting transition temperatures ≈4 K [1–3]. In the family of spinel oxides, superconductivity was first realized in the mixed valent titanate spinel $LiTi_2O_4$ [4], with the highest transition temperature (T_c) of 13.7 K [5]. While the mechanism driving the superconducting transition in $LiTi_2O_4$ still remains to be settled, the role of orbital degrees of freedom and spin-orbital fluctuations seem important [6–10]. Several investigations were performed to increase the superconducting T_c of $LiTi_2O_4$ by doping at the Ti site with Mg, Mn, Li, Al, and Cr ions, however, the T_c was found to decrease rapidly with an increase in doping percentage [11–14]. Superconductivity in the family of mixed titanate spinel oxide Mg_2TiO_4-$MgTi_2O_4$ remains controversial; in one group of studies, the Mg_2TiO_4-$MgTi_2O_4$ compounds were found to exhibit a zero resistive transition, albeit with the onset of a diamagnetic signal at much lower temperatures (almost at 40 K smaller temperatures than the onset of the zero resistance state) [15–18], and other group of studies instead suggested these compounds to be semiconducting [14,19]. Recently, superconductivity has been reported in a superlattice consisting of $MgTi_2O_4$ and $SrTiO_3$ with $T_c \approx 3$ K (where substrate-induced strain was found to play a critical role) [20] and in Mg:Ti_9O_{10} (possessing an orthorhombic Ti_9O_{10} structure) film on the (011)-oriented substrate ($MgAl_2O_4$) with $T_c \approx 5$ K [21]. Bulk $MgTi_2O_4$, containing Ti^{3+} ions, remains insulating (reported to be a Mott insulator [22,23]) down to the lowest temperature and undergoes an insulator to high-temperature metal (or semiconducting [19]) transition around 260 K. This phase transition is also accompanied with a Ti^{3+}-ion related Jahn-Teller distortion-driven tetragonal to cubic structural and a Ti spin-singlet transition [24,25]. The low-temperature tetragonal phase hosts a unique tetramer orbital ordering involving the Ti t_{2g} orbitals along the ⟨111⟩ direction and is chiral ($P4_12_12$) [22,23,26]. V-doped $MgTi_2O_4$ still remains a Mott insulator down to the lowest temperature [27,28], however, V doping leads to a unique mixed valence state for both Ti (Ti^{3+} and Ti^{4+}) and V ions (V^{3+} and V^{2+}), as it is energetically favorable for some of the Ti^{3+} ($3d^1$) ions to donate their single electron (and thereby become Jahn-Teller inactive $3d^0$) to the doped V^{3+} ($3d^2$) ions (which also then becomes Jahn-Teller inactive $3d^3$) [28]. This mixed valence state of the transition metal ions in V-doped $MgTi_2O_4$ accompanied with a unique band structure leads to exotic functional properties, such as a dc current-induced insulator to metal switching at ultralow electric field [28]. The present

*Present address: School of Physical Sciences, Indian Association for the Cultivation of Science, Jadavpur, Kolkata 700032, India.
†debraj@phy.iitkgp.ac.in

 ©2023 American Physical Society

results on the emergence of superconductivity on the surface layer of V-doped $MgTi_2O_4$, further charge doped due to Mg deficiency, with a higher T_c ($\approx$16 K) (the highest T_c among spinels) and a very high upper critical magnetic field value is thus extremely promising.

II. METHODOLOGY

To synthesize polycrystalline $MgTi_{1.4}V_{0.6}O_4$, MgO (10% excess Mg taken following Ref. [19]), TiO_2, V_2O_3, and metallic Ti powders were thoroughly mixed, ground, and cast into a pellet. The resultant pellet was subsequently annealed at 1080 °C under vacuum condition in a sealed quartz tube. While the bulk of the sample was found to be black in color (corresponding to the $MgTi_{1.4}V_{0.6}O_4$ phase), a combination of two phases could be detected as a thin-surface layer, one of them being the black-colored bulk phase and another an emergent grayish-colored phase. To investigate the structural phase of the surface layer, we have carried out grazing-incidence x-ray diffraction (GIXRD) with a very-low incident angle using a Cu $K\alpha$ source. The powder x-ray diffraction (XRD) of the bulk sample was obtained after scraping off the thin grayish surface layer to investigate the structural phase. Micro-Raman experiments were carried out using a 532-nm laser source to further investigate the structural phases of the grayish and dark regions of the thin surface layer. Temperature-dependent four-probe resistivity and magnetization measurements were carried out using a physical property measurement system (PPMS). The resistivity measurements were carried out by painting electrical contacts on the $MgTi_{1.4}V_{0.6}O_4$ sample, with and without (obtained by scraping with sandpaper) the thin grayish surface layer, as shown in the insets of Fig. 3(a).

III. RESULTS AND DISCUSSION

A. Structural properties

We first discuss the structural phases for the bulk and the grayish surface layer, as investigated through x-ray diffraction (XRD). As seen by a comparison with the XRD diffraction pattern of standard $MgTi_2O_4$ in Fig. 1(a), the bulk of the synthesized $MgTi_{1.4}V_{0.6}O_4$ is found to stabilize into a cubic spinel phase. Along with the main spinel phase, a small fraction of a secondary phase of Ti_2O_3 (corundum) (the corresponding XRD peaks are indicated by asterisks) can also be detected. Since the Ti_2O_3 is not superconducting [29,30] (also the bulk sample, without the surface layer, is found to be insulating), its presence does not affect the present results. To probe the structural phase of the surface layer, GIXRD with a very low incident grazing angle of 1.5° was performed, so that the x-ray beam mostly becomes diffracted from the surface layer. Clear, though weak (due to low sample volume), characteristic XRD peaks corresponding to two spinel phases, which vary in their lattice parameters (thereby leading to a splitting in the XRD peak positions), can be detected through GIXRD [as seen in Fig. 1(b)]. Notably, the GIXRD peaks of the thin grayish surface layer do not match with the XRD pattern corresponding to the Ti_9O_{10} orthorhombic structure of the superconducting Mg-Ti-O superconducting films [21].

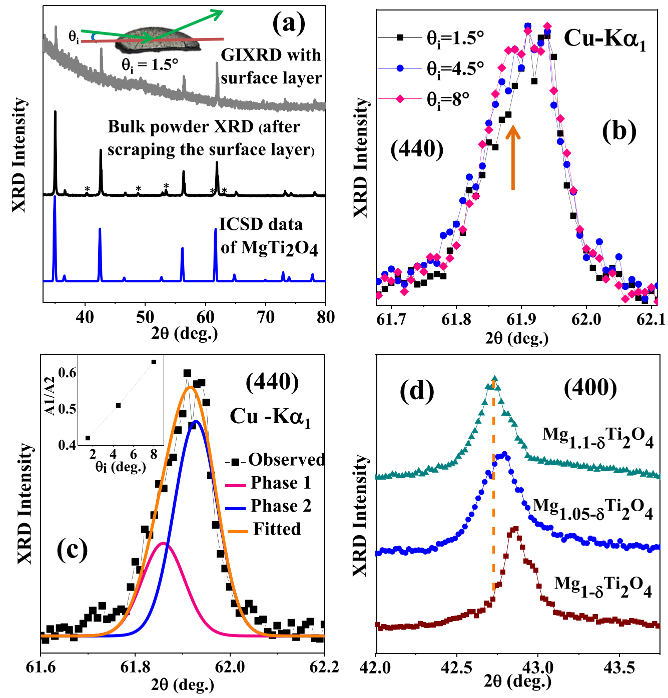

FIG. 1. (a) Comparison of powder XRD of the bulk sample (after scraping of the surface layer), GIXRD for grazing incidence (θ_i) 1.5° with the surface layer, and standard XRD data of bulk $MgTi_2O_4$ [obtained from the Inorganic Crystal Structure Database (ICSD)]. The marked asterisks in the bulk powder XRD arise from a small Ti_2O_3 secondary phase. (b) Comparison of the (440) GIXRD peak [collected using a Ge(220) 2-bounce monochromator] for different grazing incidences. (c) (440) GIXRD peak fitted with two phases. The inset shows the obtained increase in the ratio of the areas corresponding to phase 1 (A1) and phase 2 (A2) (i.e., $\frac{A1}{A2}$) with an increase in the grazing incidence angle, suggesting a relative increase in the phase 1 fraction with increasing sample depth. (d) Shifts of the (400) XRD peaks towards the lower 2θ value with an increase in Mg percentage in different $MgTi_2O_4$ samples. 10% excess Mg was taken to account for Mg volatility following Ref. [19].

The observation of two spinel phases [as seen in Fig. 1(b)] through GIXRD, is consistent with an inspection of the top grayish surface layer under a microscope (as seen in Fig. S1 of the Supplemental Material [31]), which clearly exhibit two distinct sample regions, i.e., overlapping grayish islands interspersed on relatively blackish sample regions, with the relative content of the latter increasing with depth in the sample. To further confirm the two spinel phases, we have collected the GIXRD using a Ge (220) 2-bounce monochromator (which suppresses Cu $K\alpha_2$ radiation) for different grazing incidences. The intensity of the lower 2θ peak in GIXRD [as shown in Fig. 1(b) and the inset of Fig. 1(c)] gradually increases with an increase in incidence angle (which thereby probes the structure deeper into the sample), suggesting that the higher 2θ peaks [shown in Fig. 1(c)] associated with a smaller lattice parameter (calculated lattice parameters included in Table S1 of the Supplemental Material [31]) correspond to the grayish regions of the surface layer. Further, a systematic decrease in the bulk lattice parameter [leading to a tuning of the corresponding XRD peak positions to higher angles, as

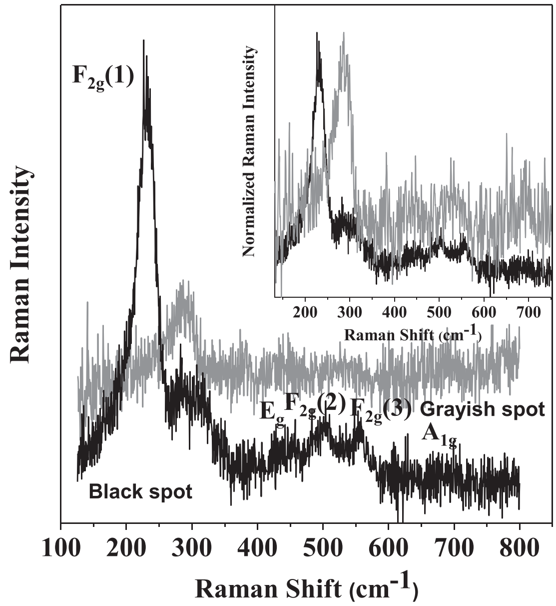

FIG. 2. Comparison of Raman spectra collected on the grayish and black regions of the thin surface layer. The inset shows normalized Raman spectra of both regions.

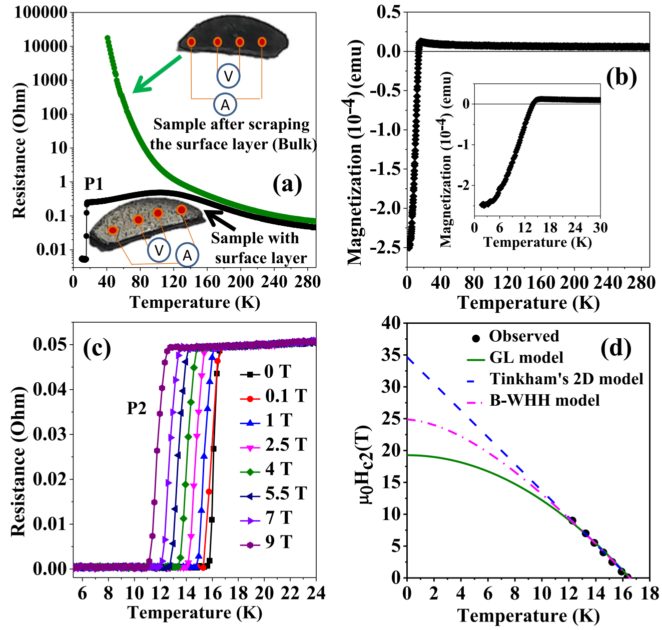

FIG. 3. (a) Comparison of temperature-dependent resistance curves of the sample with and without the grayish surface layer (the latter obtained after scraping the grayish surface layer). The surface of the sample has a different grayish color (shown in the lower inset of the figure) than the blackish bulk (the latter picture is taken after scraping the grayish surface layer and is shown in the upper inset of the figure). Temperature-dependent resistance curves of the sample with the grayish surface layer exhibiting sharp superconducting transitions, while the bulk (after scraping off the grayish surface layer) exhibits semiconducting behavior. P1 and P2 stands for different pieces of the sample. (b) Temperature dependence of magnetization, measured with 0.01 T applied magnetic field, collected following the zero-field-cooling protocol. The inset shows a zoomed view of the diamagnetic transition below the superconducting transition temperature. (c) Temperature-dependent resistance curves collected with different applied magnetic fields. (d) Fitting of the critical magnetic field data with superconducting transition temperatures with Ginzburg-Landau (GL), Werthamer-Helfand-Hohenberg (WHH), and Tinkham's 2D model.

seen in Fig. 1(d) and also Figs. S2 and S3 of the Supplemental Material [31]] on reducing the Mg content in a control $Mg_xTi_2O_4$ and V-doped $Mg_xTi_2O_4$ series is clearly observed. The spinel phase corresponding to the higher 2θ XRD peaks [seen in Fig. 1(c)] is thus likely off-stoichiometric (most likely Mg deficient due to its increased volatility at higher sintering temperature), while the spinel phase corresponding to the lower 2θ XRD peaks is near stoichiometric [comparable to the bulk, as seen in Fig. 3(a), which is black in color]. To further investigate the structural properties, micro-Raman measurements were carried out by preliminarily focusing the laser beam on the grayish and black regions of the surface layer, as shown in Fig. 2. The corresponding Raman peaks and their positions, the reproducibility of which were checked between different regions, clearly suggest spinel phases for both these regions [32–36]. The observed main peak around 230 cm^{-1} in the Raman spectra for the black region is reported to be associated with vibrations involving mainly the AO_4 (in our case with MgO_4) units of the spinel phase [33,35]. The decrease in intensity in the Raman spectra of the grayish region suggests A-site off-stoichiometry and associated disorder for the grayish surface layer. Due to a preponderance of grayish sample regions over the black sample portions (as seen in Fig. S1 of the Supplemental Material [31]) in the top layer (both having typical grain sizes of ∼1 μm, which is also comparable to the Raman laser-beam spot size), a small hump, at around 300 cm^{-1}, corresponding to the main peak of the gray sample area, becomes discernible in the Raman spectrum collected on the black sample regions, as seen in Fig. 2. However, the shift in the main peak positions (shown in the inset of Fig. 2) of the grayish region to a higher wave number in comparison to the corresponding spectra for the black region indicates a decrease in lattice parameters for the grayish region, consistent with the GIXRD results.

B. Transport and magnetic properties

The temperature-dependent four-probe resistivity values of the polycrystalline $MgTi_{1.4}V_{0.6}O_4$ sample, measured with and without the grayish surface layer, are shown in Fig. 3(a). Surprisingly, while the measurement including the grayish surface layer exhibits a superconducting transition, with a high T_c of around 16 K, the measurement on the sample without the grayish surface layer (i.e., property of the bulk of the sample) leads to an insulating behavior down to the lowest temperature. The high-temperature insulating nature, which shows a similar temperature dependency for both resistivity curves, appears to be driven by the resistivity of the bulk sample. At temperatures below around 120 K, the transport property of the grayish surface layer seems to dominate over the bulk transport property, suggesting a lower resistance for the surface layer in this temperature range. To further validate the emergence of a superconducting phase within the grayish surface layer, we have measured the temperature-dependent magnetization on the pellet sample (which included the surface layer). Expectedly, the magnetization curve, as shown in Fig. 3(b), clearly exhibits a sharp diamagnetic transition below the superconducting transition temperature of around 16 K [seen in the inset of Fig. 3(b)]. Notably, the observed T_c for the superconducting transition is found to be the highest among the family of superconducting spinel compounds [1–4,37]. The temperature-dependent resistivity curves, measured with varying applied magnetic fields, illustrates that even a high magnetic field of 9 T remains nearly ineffective in changing the sharpness of the superconducting transition [as seen in Fig. 3(c)] or the superconducting T_c substantially (T_c decreases by $\sim$ 4 K for 9 T magnetic field), thereby suggesting a very high upper critical magnetic field of this system. To estimate the critical magnetic field, the T_c (taken to be the temperature at which the resistance drops to 90% of the normal state resistance) values corresponding to different magnetic fields have been plotted and fitted with some of the proposed models of superconductivity, such as the Ginzburg-Landau [38,39], Werthamer-Helfand-Hohenberg (WHH) [40], and Tinkham's two-dimensional (2D) models [41–43], as shown in Fig. 3(d). The WHH and Tinkham's model, observed to fit the experimental data better in comparison to the Ginzburg-Landau model, suggests a very high upper critical magnetic field, such as ~25 and 35 T, respectively. Further investigations to ascertain the exact critical field value [i.e., to understand whether it is beyond the Pauli paramagnetic limit ($B_p = 1.84T_c \approx 30$ T)] will necessitate resistivity measurements with higher magnetic field values. Notably, both the estimated upper critical field values are much higher than those reported for either the sulfo- and selenide superconductors (with upper critical magnetic field values of less than 5 T [1–3]) or the spinel oxide superconductors ($LiTi_2O_4$ and superlattices of $MgTi_2O_4$, which have an upper critical field value ≈12 T [6,20,21,44]). Thus, the emergence of superconductivity in this system not only leads to the highest T_c among spinel compounds but is also associated with a very high upper critical magnetic field, which is promising. Nonsuperconducting precipitates (the darker regions of the surface layer), that naturally occur on the surface layer of V-doped $Mg_{1-x}Ti_2O_4$ along with the superconducting regions, likely act as very efficient pinning centers for the superconducting vortices. Such pinning centers often are artificially engineered to make the irreversibility magnetic field values (above which the dissipationless transport or critical-current value vanishes) come close to the critical magnetic field (H_{c2}) values, which is essential for applications [45–47]. The irreversibility magnetic field values of the V-doped $Mg_{1-x}Ti_2O_4$, as probed using current (I)-voltage (V) characteristics [shown in Fig. 4(a) and Fig. S5 of the Supplemental Material [31]] are estimated to be very close to the corresponding H_{c2} values [as shown in Figs. 4(b) and 3(d)], further highlighting the promise of this superconducting system. The realization of strained $MgTi_2O_4$ in a thin-film superlattice with $SrTiO_3$ was reported to be crucial for the onset of superconductivity in $MgTi_2O_4$, albeit with a much lower T_c and upper critical magnetic field values of ~3 K and 12 T, respectively [20]. While a decrease in lattice parameter for the grayish region, aided through Mg off-stoichiometry (which also dopes charge carriers), is naturally realized here (as suggested through GIXRD, Raman,

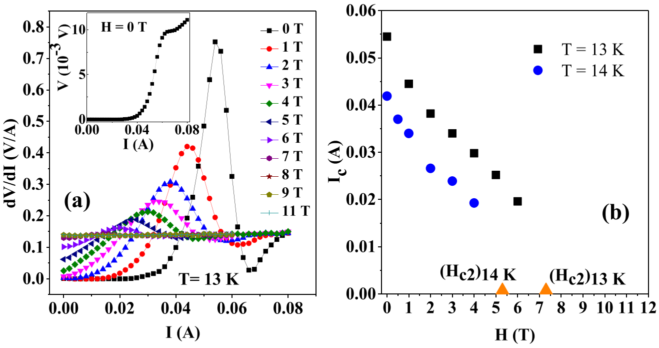

FIG. 4. (a) Isothermal $\frac{dV}{dI}$ vs I curve at 13 K for various applied magnetic field values. The inset shows the corresponding V-I curve in the absence of an applied magnetic field. (b) Magnetic field dependence of the critical currents [determined from the current value associated with a peak in the corresponding $\frac{dV}{dI}$ curve, as shown in (a)] at 13 and 14 K. The upper critical magnetic field [determined from the resistance data of Fig. 3(d)] corresponding to 13 and 14 K are also indicated by solid triangles.

and energy-dispersive x-ray investigations [31,48–51]), the role of V doping also seems very important. Particularly, as discussed earlier, V doping into $MgTi_2O_4$ does bring in charge and orbital fluctuations, and whether it helps in boosting superconductivity remains to be investigated. Triggered by our initial submission of these results to the [52], a recent density-functional-based study [53] has investigated the role of Mg deficiency and reduced Jahn-Teller activity (arising from a mixed valence of V and Ti ions, as also shown in Ref. [28]) towards superconducting instability in a V-doped $MgTi_2O_4$ system.

IV. SUMMARY

In summary, we have reported the emergence of superconductivity on a surface layer of a V-doped $MgTi_2O_4$ sample. The superconducting transition temperature and upper critical magnetic field is found to be five times and two times enhanced as compared to $MgTi_2O_4$ and $SrTiO_3$ superlattices. The sample off-stoichiometry (Mg deficiency for the spinel phase of the surface layer) along with the doping of V ions seem critical for the observed superconductivity.

ACKNOWLEDGMENTS

A.R. would like to acknowledge functional material laboratory members, IIT Kharagpur, for their help and support. D.C. acknowledges financial support from INSA Young Scientist project Grant No. INSA/SP/YSP/151/2018/233. T.P. would like to acknowledge SERB for providing support through a fellowship (file No. PDF/2016/002580). A.N.P. acknowledges financial support from DST-Nano Mission Grant No. DST/NM/TUE/QM-10/2019. The authors acknowledge the characterization facilities from the TRC project of SNBNCBS. The authors acknowledge support from Ministry of Electronics and Information Technology (MeitY) No. 5(7)/2017-NANO 5(1)/2021-NANO, and would like to thank Professor Anushree Roy, Professor Atsushi Fujimori, and Professor Arghya Taraphder for helpful discussions.

[1] T. Hagino, Y. Seki, N. Wada, S. Tsuji, T. Shirane, K. Kumagai, and S. Nagata, Phys. Rev. B **51**, 12673 (1995).
[2] H. Luo, Y. Klimczuk, L. Müchler, L. Schoop, D. Hirai, M. K. Fuccillo, C. Felser, and R. J. Cava, Phys. Rev. B **87**, 214510 (2013).
[3] Y. He, Y. X. You, L. Zeng, S. Guo, H. Zhou, K. Li, Y. Huang, P. Yu, C. Zhang, C. Cao, and H. Luo, Phys. Rev. B **105**, 054513 (2022).
[4] D. C. Johnston, H. Prakash, W. H. Zachariasen, and R. Viswanathan, Mater. Res. Bull. **8**, 777 (1973).
[5] D. C. Johnston, J. Low Temp. Phys. **25**, 145 (1976).
[6] C. P. Sun, J.-Y. Lin, S. Mollah, P. L. Ho, H. D. Yang, F. C. Hsu, Y. C. Liao, and M. K. Wu, Phys. Rev. B **70**, 054519 (2004).
[7] K. Jin, G. He, X. Zhang, S. Maruyama, S. Yasui, R. Suchoski, J. Shin, Y. Jiang, H. S. Yu, J. Yuan, L. Shan, F. V. Kusmartsev, R. L. Greene, and I. Takeuchi, Nat. Commun. **6**, 7183 (2015).
[8] Z. Wei, G. He, W. Hu, Z. Feng, X. Wei, C. Y. Ho, Q. Li, J. Yuan, C. Xi, Z. Wang, Q. Chen, B. Zhu, F. Zhou, X. Dong, L. Pi, A. Kusmartseva, F. V. Kusmartsev, Z. Zhao, and K. Jin, Phys. Rev. B **100**, 184509 (2019).
[9] E. G. Moshopoulou, J. Am. Ceram. Soc. **82**, 3317 (1999).
[10] Y. Jia, G. He, W. Hu, H. Yang, Z. Yang, H. Yu, Q. Zhang, J. Shi, Z. Lin, J. Yuan, B. Zhu, L. Gu, H. Li, and K. Jin, Sci. Rep. **8**, 3995 (2018).
[11] P. M. Lambert, M. R. Harrison, and P. P. Edwards, J. Solid State Chem. **75**, 332 (1988).
[12] P. M. Lambert, P. P. Edwards, and M. R. Harrison, J. Solid State Chem. **89**, 345 (1990).
[13] M. R. Harrison, P. P. Edwards, and J. B. Goodenough, Philos. Mag. B **52**, 679 (1985).
[14] K. Isawa, J. Sugiyama, and H. Yamauchi, Phys. Rev. B **49**, 1462 (1994).
[15] T. J. Cogle, C. A. S. Mateus, J. H. Binks, and J. T. S. Irvine, J. Mater. Chem. **1**, 289 (1991).
[16] C. Namgung, A. B. Sheikh, A. A. Finch, and J. T. S. Irvine, Appl. Supercond. **1**, 511 (1993).
[17] A. B. Sheikh, A. A. Finch, C. C. Mather, and J. T. S. Irvine, Phys. C: Supercond. **212**, 95 (1993).
[18] A. A. Finch, A. B. Sheikh, G. Mather, C. Namgung, and J. T. S. Irvine, in *Advances in Superconductivity V*, edited by Y. Bando and H. Yamauchi (Springer, Tokyo, 1993), p. 255.
[19] H. D. Jhou and J. B. Goodenough, Phys. Rev. B **72**, 045118 (2005).
[20] W. Hu, Z. Feng, B. C. Gong, G. He, D. Li, M. Qin, Y. Shi, Q. Li, Q. Zhang, J. Yuan, B. Zhu, K. Liu, T. Xiang, L. Gu, F. Zhou, X. Dong, Z. Zhao, and K. Jin, Phys. Rev. B **101**, 220510(R) (2020).
[21] Z. Ni, W. Hu, Q. Zhang, Y. Zhang, P. Xiong, Q. Li, J. Yuan, Q. Chen, B. Zhu, H. Zhang, X. Dong, L. Gu, and K. Jin, Phys. Rev. B **105**, 214511 (2022).
[22] S. Leoni, A. N. Yaresko, N. Perkins, H. Rosner, and L. Craco, Phys. Rev. B **78**, 125105 (2008).
[23] S. Di Matteo, G. Jackeli, C. Lacroix, and N. B. Perkins, Phys. Rev. Lett. **93**, 077208 (2004).
[24] M. Schmidt, W. Ratcliff II, P. G. Radaelli, K. Refson, N. M. Harrison, and S. W. Cheong, Phys. Rev. Lett. **92**, 056402 (2004).
[25] M. Isobe and Y. Ueda, J. Phys. Soc. Jpn. **71**, 1848 (2002).
[26] D. I. Khomskii and T. Mizokawa, Phys. Rev. Lett. **94**, 156402 (2005).
[27] W. Sugimoto, H. Yamamoto, Y. Sugahara, and K. Kuroda, J. Phys. Chem. Solids **59**, 83 (1998).
[28] A. Rahaman, T. Paramanik, R. K. Maurya, K. Yadav, R. Bindu, K. Mukherjee, and D. Choudhury, Phys. Rev. B **103**, 245145 (2021).
[29] F. J. Morin, Phys. Rev. Lett. **3**, 34 (1959).
[30] C. F. Chang, T. C. Koethe, Z. Hu, J. Weinen, S. Agrestini, L. Zhao, J. Gegner, H. Ott, G. Panaccione, H. Wu, M. W. Haverkort, H. Roth, A. C. Komarek, F. Offi, G. Monaco, Y.-F. Liao, K.-D. Tsuei, H.-J. Lin, C. T. Chen, A. Tanaka, and L. H. Tjeng, Phys. Rev. X **8**, 021004 (2018).
[31] See Supplemental Material at http://link.aps.org/supplemental/10.1103/PhysRevB.107.245124 for additional structural and transport analysis.
[32] Z. Wang, H. S. C. O' Neill, P. Lazor, and S. K. Saxena, J. Phys. Chem. Solids **63**, 2057 (2002).
[33] L. Malavasi, P. Galinetto, M. C. Mozzati, C. B. Azzoni, and G. Flor, Phys. Chem. Chem. Phys. **4**, 3876 (2002).
[34] V. D'Ippolito, G. B. Andreozzi, D. Bersaniband, and P. P. Lottici, J. Raman Spectrosc. **46**, 1255 (2015).
[35] M. Singha, B. Paul, and R. Gupta, J. Appl. Phys. **127**, 145901 (2020).
[36] Z. V. Popović, G. De Marzi, M. J. Konstantinović, A. Cantarero, Z. Dohčević-Mitrović, M. Isobe, and Y. Ueda, Phys. Rev. B **68**, 224302 (2003).
[37] Y. Okada, Y. Ando, R. Shimizu, E. Minamitani, S. Shiraki, S. Watanabe, and T. Hitosugi, Nat. Commun. **8**, 15975 (2017).
[38] M. Cyrot, Rep. Prog. Phys. **36**, 103 (1973).
[39] B. Rosenstein and D. Li, Rev. Mod. Phys. **82**, 109 (2010).
[40] N. R. Werthamer, K. Helfand, and P. C. Hohenberg, Phys. Rev. **147**, 295 (1966).
[41] M. Tinkham, Phys. Rev. **129**, 2413 (1963).
[42] R. H. White and M. Tinkham, Phys. Rev. **136**, A203 (1964).
[43] F. E. Harper and M. Tinkham, Phys. Rev. **172**, 441 (1968).
[44] L. Tang, P. Y. Zou, L. Shan, A. F. Dong, G. C. Che, and H. H. Wen, Phys. Rev. B **73**, 184521 (2006).
[45] A. Gurevich, Nat. Mater. **10**, 255 (2011).
[46] S. Lee, J. Jiang, J. D. Weiss, C. M. Folkman, C. W. Bark, C. Tarantini, A. Xu, D. Abraimov, A. Polyanskii, C. T. Nelson, Y. Zhang, S. H. Baek, H. W. Jang, A. Yamamoto, F. Kametani, X. Q. Pan, E. E. Hellstrom, A. Gurevich, C. B. Eom, and D. C. Larbalestier, Appl. Phys. Lett. **95**, 212505 (2009).
[47] J. Jaroszynski, F. Hunte, L. Balicas, Y.-J. Jo, I. I. Raičević, A. Gurevich, D. C. Larbalestier, F. F. Balakirev, L. Fang, P. Cheng, Y. Jia, and H. H. Wen, Phys. Rev. B **78**, 174523 (2008).
[48] A. Kitada, A. M. Arevalo-Lopezb, and J. P. Attfield, Chem. Commun. **51**, 11359 (2015).
[49] E. Moshopoulou, P. Bordet, A. Sulpice, and J. J. Capponi, Phys. C: Supercond. **235-240**, 747 (1994).
[50] L. A. de Picciotto and M. M. Thackeray, J. Power Sources **35**, 323 (1991).
[51] R. Basso, S. Carbonin, and A. Della Giusta, Z. Kristallogr. **194**, 111 (1991).
[52] A. Rahaman, T. Paramanik, B. Pal, R. Pal, P. Maji, K. Bera, S. Mallik, D. K. Goswami, A. N. Pal, and D. Choudhury, arXiv:2209.02053.
[53] D. Dey, T. Maitra, and A. Taraphder, Phys. Rev. B **107**, 174515 (2023).